J IRAN CHEM SOC (2015) 12:537–549
DOI 10.1007/s13738-014-0511-x

ORIGINAL PAPER

Multi SO_3H supported on carbon nanotubes: a practical, reusable, and regioselective catalysts for the *tert*-butylation of *p*-cresol under solvent-free conditions

Reza Fareghi-Alamdari · Mohsen Golestanzadeh · Negar Zekri · Zeinab Mavedatpoor

Received: 10 February 2014 / Accepted: 18 July 2014 / Published online: 24 August 2014

Abstract The present study describes the synthesis, characterization, and catalytic activity of sulfonated multi-walled carbon nanotubes and sulfonated single-walled carbon nanotubes in the *tert*-butylation of *p*-cresol. The catalysts were prepared using a chemical and simple process and it characterized by scanning electron microscopy, Fourier transform infrared, and Raman spectroscopy, thermogravimetric analysis, and acid–base titration. The sulfonated multi-walled carbon nanotubes and sulfonated single-walled carbon nanotubes have been used as practical heterogeneous catalytic systems in the *tert*-butylation of *p*-cresol under solvent-free conditions. Sulfonated multi-walled carbon nanotubes with the highest total density of SO_3H groups possessed high activity for *p*-cresol conversion and high selectivity than the sulfonated single-walled carbon nanotubes. This methodology offers some advantages of high selectivity, and high yields, easy work-up, solvent-free conditions, and reusable catalyst. Moreover, the catalytic system was used in scale-up under similar optimized reaction conditions.

Keywords Carbon nanotube · *p*-Cresol · Solid acid · *Tert*-butylation · Solvent-free

Introduction

In the recent years, the exploration for new developments in the chemical industries and environmentally benign chemical processes or methodologies has received increasing attention due to their role in safety, energy efficiencies, and conservation of the global ecosystem [1]. In this regard, owing to the simplified recovery and reusability, the use of heterogeneous catalysts is frequently superior for many chemical reactions surrounded by both academic and industrial setting [2]. However, in addition to reusability, one of the most important desiderata in the field of sustainable chemistry is the replacement of the toxic and unstable catalysts by safer analogs accompanied with employing renewable and more accessible energy sources while demonstrating similar or even higher levels of activity. Along this line, carbon based catalysts comprising carbon nanotubes (CNTs) have been recognized as promising tools to attain this goal in organic transformations [3–9]. Due to the high specific surface area of CNTs, they are effective supports for immobilization of active species for the synthesis of solid acid catalysts. Recently, the sulfonated carbon nanotubes (CNTs-SO_3H) have been achieved by some reported methods [10–15]. The covalent functionalization of CNTs with sulfonic acid groups provides stability, considerable solubility and strong surface acidity. The CNTs-SO_3H is useful as solid acid catalyst in organic reactions.

The synthesis of bulky organic molecules is an important area of search for industrial purpose. The *tert*-butylated benzene derivatives, typically bulky molecules are commercially important chemical intermediates. They have been used for the synthesis of antioxidants, antiseptics, agrochemicals, resins, UV absorber and stabilizer for the polymers [16–18]. *Tert*-butylated benzene derivatives, especially 2-*tert*-butyl-*p*-cresol (2-TBC) are widely employed for the synthesis of antioxidants such as 2,2′-methylene-bis-(6-*tert*-butyl-*p*-cresol) (A.O.2246). The chemical structures of some antioxidants are shown in Fig. 1.

R. Fareghi-Alamdari (✉) · N. Zekri · Z. Mavedatpoor
College of Chemistry and Chemical Engineering, Malek-Ashtar University of Technology, 16765-3454 Tehran, Iran
e-mail: reza_fareghi@yahoo.com

M. Golestanzadeh
Department of Organic Chemistry, Faculty of Chemistry, University of Kashan, 87317-51167 Kashan, Iran

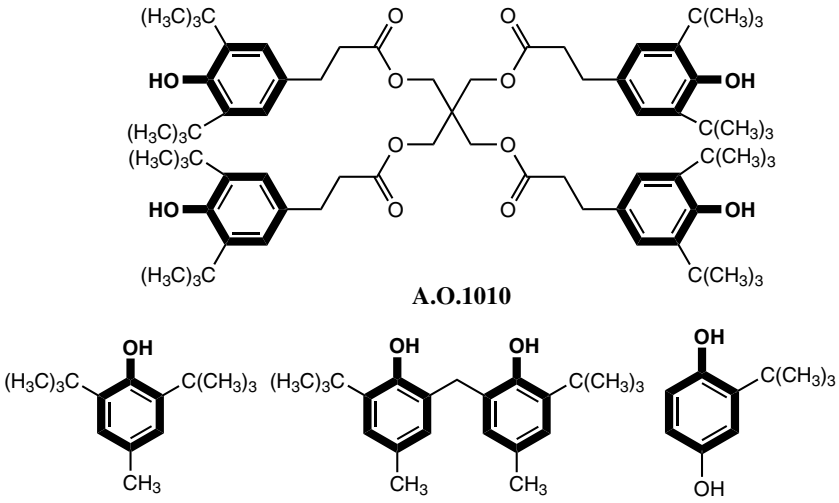

Fig. 1 Selected example of some important phenolic antioxidants

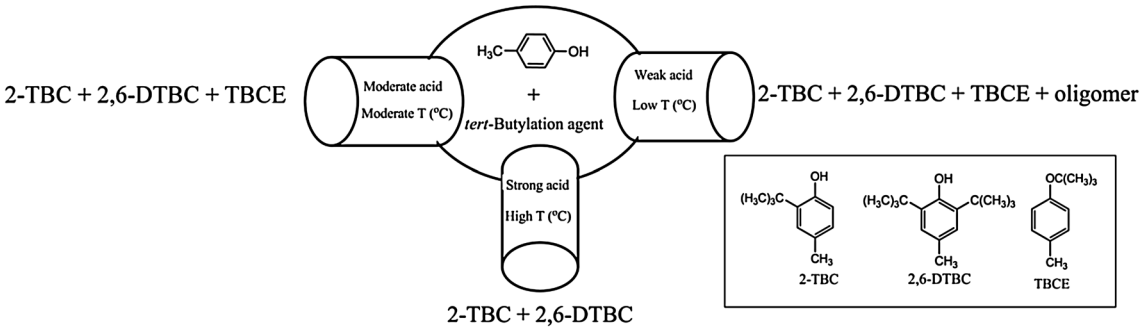

Scheme 1 Products distribution in the *tert*-butylation of *p*-cresol under different conditions

Owing to the importance of the described compounds, extensive studies have been carried out on the *tert*-butylation of phenol derivatives over heterogeneous catalysts such as [H-Al-MCM-48] [19], [K–Fe-10] [20], Zeolites [21–27], [Fe–Al-MCM-41] [28], $Cu_{0.5}Co_{0.5}Fe_2O_4$ [29],X-SBA-15 [30, 31], [X-MCM-41-SO_3H] [32–34], Ionic liquids-SO_3H [35–38], RHAPhSO_3H [39], TPA-TiO_2 [40], X-ZrO_2 [41–46], HPW-MCM-41 [47], Zn-Al-MCM-41 [48],[Al-MCM-41] [49], and homogeneous catalysts such as brØnsted acids, (H_2SO_4, HF, H_3PO_4, and $HClO_4$) and Lewis acids ($AlCl_3$ and BF_3) [50, 51].

Since the catalytic activity and selectivity of *tert*-butylation of phenol derivatives are highly depended to the used catalyst and reaction conditions, unfortunately some of the reported methods have drawbacks. Some of these most important disadvantages associated with the current methods are equipment corrosion, environmental pollution, and use of toxic organic solvents, production of waste, low selectivity and yield, non-reusable catalyst and rapid deactivation of the catalysts. Therefore, it is an important task to find suitable catalysts for the synthesis of these bulky alkylated phenols as a green chemical technology. As shown in Scheme 1, different products of *tert*-butylation of *p*-cresol present depend upon the strength of the acid sites, temperature and other reaction conditions.

Recently, we studied the catalytic activity and selectivity of nano$Cu_{1-x}Co_xFe_2O_4$in the liquid phase *tert*-butylation of *p*-cresol with methyl-*tert*-butyl ether (MTBE) [52]. In continuation of our interest toward application of nanocatalysts in organic reactions [53–55], we decided to investigate the possibility of utilization of CNTs-SO_3H in the *tert*-butylation of *p*-cresol.

Experimental

Materials and apparatus

The CNTs used in this study [SWCNTs: (L = 20–30 μm, D = 1–3 nm)] [MWCNT: (L = 25–35 μm, D = 15–20 nm)] have been purchased from Research Institute of Petroleum Industry (RIPI-Iran). The chemicals used in this

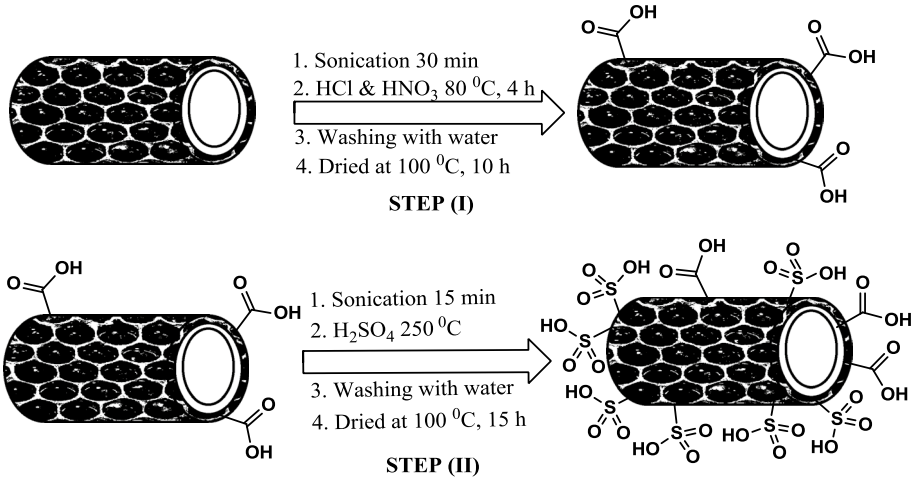

Scheme 2 Synthetic route for preparation of the catalyst (MWCNTs-SO_3H & SWCNTs-SO_3H)

work were purchased from Aldrich and Merck chemical companies. All reactions were carried out under magnetic stirring in a 25 mL glass reactor. IR spectra were obtained with KBr pellets in the range of 400–4,000 cm^{-1} with a Nicolet-860 spectrometer. NMR spectra were recorded in $CDCl_3$ solvent on a Brucker 250 MHz spectrometer DPX-3300 using tetramethylsilane (TMS) as an internal standard. The Raman spectra were recorded with an Almega Thermo Nicolet Dispersive Raman spectrometer excited at 532 nm. Thermogravimetric analysis (TGA) was performed on a mettle TA 4000 instrument at a heating rate of 10 °C min^{-1} under nitrogen atmosphere. SEM images of CNTs were taken on a Philips XL30 SEM instrument. The identity of the products was confirmed by gas chromatography (GC, HP-5890) equipped with a capillary column.

Preparation of the catalysts

In a typical experiment, multi-walled carbon nanotubes (MWCNTs) (1 g) and 100 mL deionized water were added in a becher and it sonicated for 30 min. After the sonication, the solvent was removed under reduced pressure and the obtained MWCNTs were transferred to another flask containing [hydrochloric acid (37 %), 25 mL; nitric acid (63 %), 25 mL] and stirred at 80 °C for 4 h under a nitrogen atmosphere. Then the solution was filtered under reduced pressure and the obtained materials were first washed thoroughly with deionized water and then dried at 100 °C for 10 h. In this step (**I**), the MWCNTs-COOH was obtained. After the step (**I**), the MWCNTs-COOH (1 g) and 50 mL deionized water were sonicated for 15 min. Then, the water was filtered and 40 mL H_2SO_4 (98 %) was added to the set-up at 250–270 °C (H_2SO_4 boils at 335 °C) for 20 h under a nitrogen atmosphere. After cooling the solution to room temperature, the solution was filtered and washed completely with deionized water for several times. The solid obtained materials dried at 100 °C for 15 h. These steps are described in Scheme 2. The sulfonated single-walled carbon nanotubes (SWCNTs-SO_3H) were prepared by same procedure.

General procedure for the ***tert-butylation of p-cresol catalyzed by CNTs-SO_3H under solvent-free conditions

In a 25 mL flask equipped with a condenser and magnetic stirring bar, a mixture of *p*-cresol (5 mmol, 0.541 g), MTBE (7.5 mmol, 0.661 g) and MWCNTs-SO_3H (30 mg) was heated at 90 °C under solvent-free conditions for 10 h. The progress of the reaction was monitored by GC. After completion of the reaction, acetone (2 × 10 mL) was added. The catalyst was filtered by simple filtration under reduced pressure. The obtained liquid was heated by evaporation on a rotary evaporator and the remained yellow compound was purified on a silica gel column (*n*-hexane: EtOAc/5:1) for the separation of 2-TBC, 2,6-di-*tert*-butyl-*p*-cresol (2,6-DTBC) and other byproducts. The identity of the desired product was performed by FT-IR and FT-NMR spectral data. The same experiment was performed by use of SWCNTs-SO_3H (35 mg).

Spectral data of 2-TBC

2-TBC: white crystal, mp 50–52 °C, FT-IR (KBr):υ (cm^{-1}) = 3,620, 3,415, 2,960, 2,875, 1,480, 1,440, 1,370, 1,235, 870. ^{1}H-NMR (250 MHz, $CDCl_3$):δ_H (ppm): 6.5–7.24 (m, *3H*, Ar), 4.58 (s, *1H*, OH), 2.26 (s, *3H*, CH_3), 1.39 (s, *9H*, ter-butyl). ^{13}C-NMR, (62.5 MHz, $CDCl_3$): δ_C(ppm): 151.9, 135.8, 129.6, 127.8, 127.2, 116.4, 34.4, 29.6, and 20.8.

Recycling of the catalyst

The reusability of the catalyst was investigated in the reaction of *p*-cresol and MTBE. After completion of the reaction, the catalyst was separated by simple filtration, and

then washed exhaustively with chloroform, deionized water and ethanol, and it dried at 80 °C for 10 h before being used with fresh *p*-cresol and MTBE. The catalyst can be reused for 5 runs without efficient loss of its catalytic activity.

The acid–base titration of the catalyst

The acidic capacity of the CNTs-SO_3H catalysts was investigated by an acid–base titration method [56, 57]. First 100 mg of MWCNTs-SO_3H dispersed in water and sonicated in a water bath for 10 min under nitrogen atmosphere to degas CO_2. Next 10 mL of NaOH (0.098 N) was added and the mixture stirred for 2 h at room temperature. Subsequently, the mixture was filtered through sintered glass (G-4) and washed several times with deionized water. The filtrate was then titrated with HCl (0.1 N) until reaching the neutral point as monitored by phenolphthalein as indicator.

Results and discussions

Preparation of the catalyst

The MWCNTs-SO_3H and SWCNTs-SO_3H were synthesized in two steps as described in Scheme 2. First, the CNTs which are commercially available were converted to CNTs-COOH with HCl (37 %) and HNO_3 (63 %). This step was carried out in order to increase the reactivity and purity of the CNTs and to remove amorphous carbon, fullerene and catalyst particles such as iron, cobalt and nickel. This step also introduced oxygen containing groups, mainly carboxyl groups on the CNTs [58, 59].After this step, H_2SO_4 (98 %) was reacted with CNTs-COOH to afford the CNTs-SO_3H.

Characterization of the MWCNTs-SO_3H and SWCNTs-SO_3H

The prepared catalysts were characterized by scanning electron microscopy (SEM), Fourier transform infrared (FT-IR) and Raman spectroscopies, thermogravimetric analysis (TGA) and acid–base titration.

SEM images of the catalysts

The SEM images of MWCNTs before and after the H_2SO_4 treatment are shown in Fig. 2. The SEM images of MWCNTs (Fig. 2a) and MWCNTs-SO_3H (Fig. 2b) indicate that the functional groups such as hydroxyl, sulfonic and carboxylic acid have been anchored to the MWCNTs. Compared with the pristine MWCNTs, the MWCNTs-SO_3H

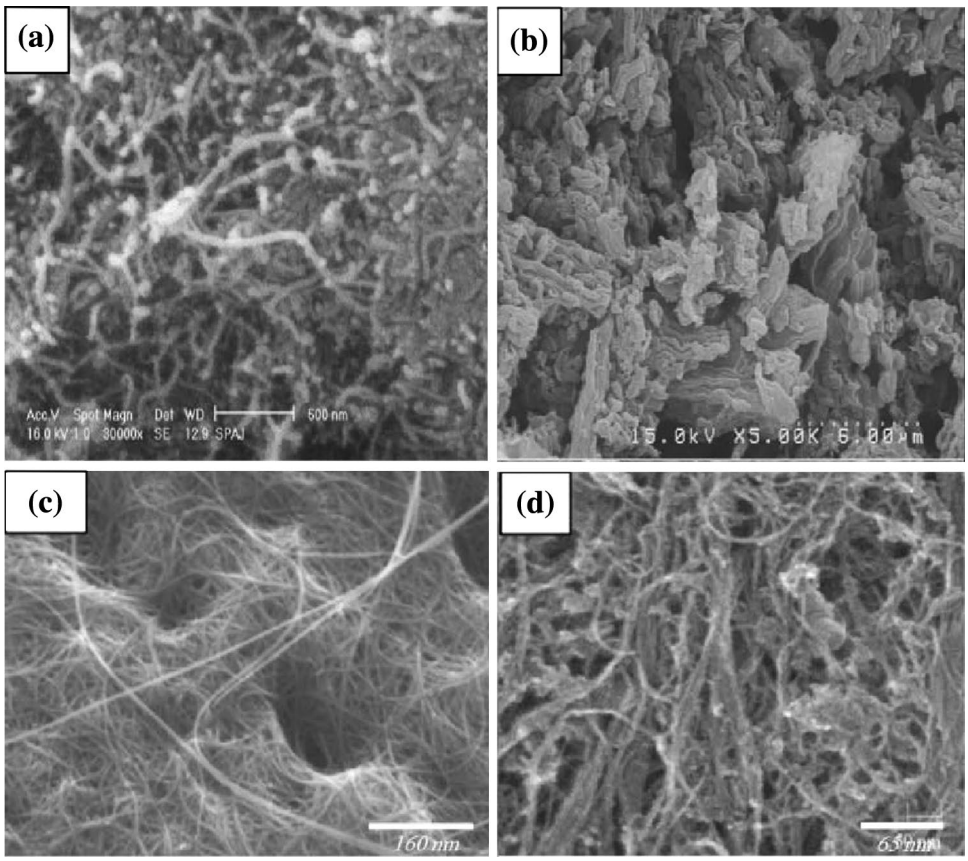

Fig. 2 SEM images of **a** MWCNTs (normal magnification), **b** MWCNTs-SO_3H (high magnification), **c** SWCNTs (normal magnification), **d** SWCNTs-SO_3H (high magnification)

was covered by a layer of foreign matter, resulting in thickened MWCNTs bundles and a denser network of nanotubes. In addition, the SEM images of SWCNTs (Fig. 2c) and SWCNTs-SO_3H (Fig. 2d) are shown in Fig. 2. The observed morphologies, by SEM images, show significant difference between SWCNTs and SWCNTs-SO_3H. It can be attributed to the presence of –OH; –COOH and –SO_3H groups on the side wall of the SWCNTs which can form hydrogen-bond-type interactions.

FT-IR studies of the catalysts

FT-IR spectra of the catalysts confirmed that functionalization of the CNTs is performed with hydroxyl, carboxylic and sulfonic acids. Figure 3 shows the FT-IR spectra of pristine CNTs, CNTs-COOH and CNTs-SO_3H of two types of the catalyst. The high symmetry presented on pristine MWCNTs and SWCNTs generates very weak infrared signals, due to the weak difference of charge states and very small induced electric dipole. The peaks related to C=C double bond at approximately 1,500 cm^{-1} for MWCNTs (Fig. 3a) and 1,550 cm^{-1} for SWCNTs (Fig. 3d) are not seen in the spectra [58].The functionalization of the CNTs with sulfonic and carboxylic acids breaks the symmetry of the CNTs, which enhances the generation of induced electric dipoles and signs as detected. Fig. 3b, e depicts MWCNTs-COOH and SWCNTs-COOH respectively. FT-IR spectrum of the MWCNTs-COOH (Fig. 3b) shows peaks at around 1,700 cm^{-1} [58], which could be assigned to C=O stretching mode of the COOH group. In Fig. 3e, another band that becomes more prominent is the one at about 1,720 cm^{-1}, which can be assigned to the carbonyl group of the carboxylic acid group attached to the end and side wall of the SWCNTs. The HNO_3: HCl oxidation process introduces not only carboxylic acid, but also alcohol or ketone species [60]. In the Fig. 3b, c weak band at approximately 1,150 $cm^{-1}$is due to the C–O stretching mode in alcoholic group [61]. Also, Fig. 3c, f shows IR spectra of MWCNTs-SO_3H and SWCNTs-SO_3H respectively. In Fig. 3c (MWCNTs-SO_3H), the broadband centered at about 3,297 cm^{-1} is resulted from the OH stretching mode of COOH and SO_3H groups [61]. In the spectrum of SWCNTs-SO_3H (Fig. 3f) this band presented at approximately 3,300 cm^{-1}. H_2SO_4 treatment with MWCNTs-COOH also results in the appearance of peaks at about 1,300 and 1,120 cm^{-1} (Fig. 3c), which corresponds to the SO_2 asymmetric and symmetric stretching modes respectively. In addition, in the low frequency part of spectrum the peak at 550 cm^{-1} was assigned to the C–S stretching mode, suggesting the existence of covalent sulfonic acid groups (Fig. 3c). The presence of the sulfonic acid group in the side wall of the SWCNTs-SO_3H (Fig. 3f) is also demonstrated by the bands at 1,120, 1,300 and 590 cm^{-1}, which correspond to the symmetric, asymmetric SO_2 and C–S stretching modes respectively.

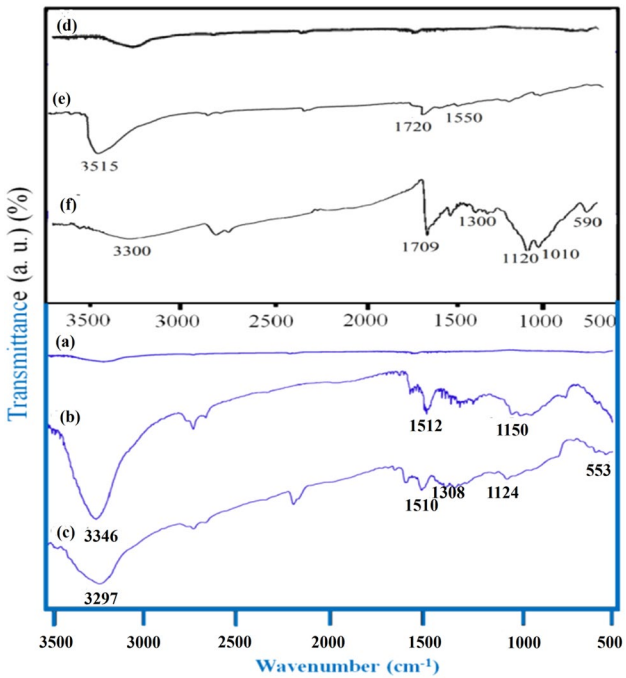

Fig. 3 FT-IR spectra of *a* MWCNTs, *b* MWCNTs-COOH, *c* MWCNTs-SO_3H, *d* SWCNTs, *e* SWCNTs-COOH, *f* SWCNTs-SO_3H

Raman spectroscopy studies of the catalysts

Raman spectroscopy is a technique frequently used to characterize CNTs [62]. In the region spectrum (1,300–1,600 cm^{-1}), two bands are observed showing the characteristic of the CNTs. These bands point the graphite band (G-band) and disorder and defects of the structure, named (D-band). The ratio between the intensity of the D-band and the G-band, noted $I_{D/G}$ value, corresponds to a higher proportion of ***sp^3 carbon [63]. These features are very useful for characterizing functionalized CNTs. Fig. 4a–f presents the Raman spectra of the two types of the catalysts and Fig. 4a–c illustrates the Raman spectra of MWCNTs, MWCNTs-COOH and MWCNTs-SO_3H respectively. As shown in Fig. 4a, the spectrum exhibits two peaks near to 1,320 and 1,571 cm^{-1}, of which the peak in 1,571 cm^{-1} is identified with the tangential mode (G-band). Also, the origin of the peak at 1,320 cm^{-1} is the D-band and its appearance has been tentatively assigned to a symmetry lowering effect, such as the presence of iron, cobalt and nickel (during synthesis of CNTs) and functional groups such as hydroxyl, sulfonic and carboxylic acid on the side walls of MWCNTs. The calculated I_D/I_G values of MWCNTs, MWCNTs-COOH and MWCNTs-SO_3H are 0.24, 0.37 and 0.84, respectively. This increasing value implies that a strong damage to the side walls of the MWCNTs is due

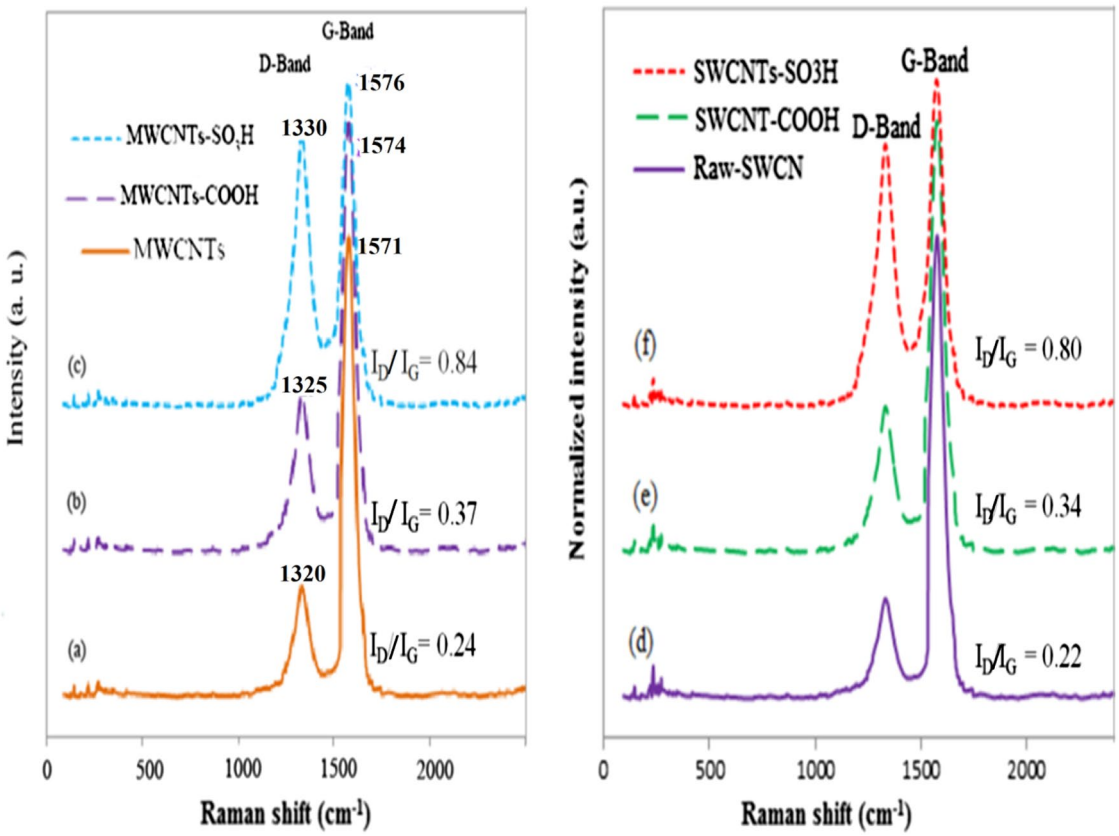

Fig. 4 Raman spectra of *a* MWCNTs, *b* MWCNTs-COOH, *c* MWCNTs-SO_3H, *d* SWCNTs, *e* SWCNTs-COOH, *f* SWCNTs-SO_3H

to the functionalized groups. These values for SWCNTs, SWCNTs-COOH and SWCNTs-SO_3H (Fig. 4d–f) are 0.22, 0.34 and 0.80 respectively. In according to the two features in the Raman spectra (D-band and G-band) we make sure that two types of the catalysts are functionalized.

Third important region in the Raman spectrum of the CNTs is radial breathing mode (RBM). The RBM region is in the low frequency of the spectrum. The Fig. 5a shows the atomic vibration of the carbon atoms in the radial direction,

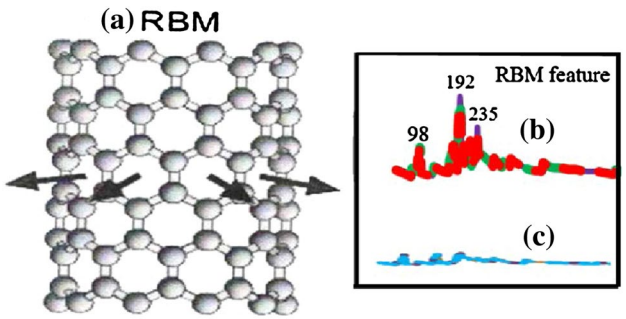

Fig. 5 *a* Atomic vibration of RBM feature in CNTs, *b* RBM feature of SWCNTs (overlapping of three sample), *c* RBM feature of MWCNTs

as if the tube was breathing. The RBM features are very useful for characterizing nanotube diameter through the Eq. (1), where the A and B parameters are determined experimentally and d_t is diameter of the CNTs [62]. For SWCNTs bundles have been found that $A = 234\ \mathrm{cm}^{-1}$ nm and $B = 10\ \mathrm{cm}^{-1}$ (where B is an upshift coming from tube–tube interaction). For more information, for isolated SWCNTs these parameters are $A = 248\ \mathrm{cm}^{-1}$ nm and $B = 0\ \mathrm{cm}^{-1}$. The diameters of SWCNTs used in this research were between 1.04 and 2.66 nm (Fig. 5b). For large diameters, tubes such as MWCNTs the intensity of the RBM features is weak or very weak and is hardly observable (Fig. 5c).

$$\omega_{\mathrm{RBM}} = \frac{A}{d_t} + B \tag{1}$$

TGA studies of the catalysts

TGA thermograms were used to determine the amount of formed sulfonic and carboxylic acid groups on the side wall of the CNTs. Figure 6a–d shows thermograms of CNTs-COOH, and CNT-SO_3H for two types of the catalysts. The weight loss between 100 and 200 °C is entirely due to the presence of amorphous carbon, water, metals and

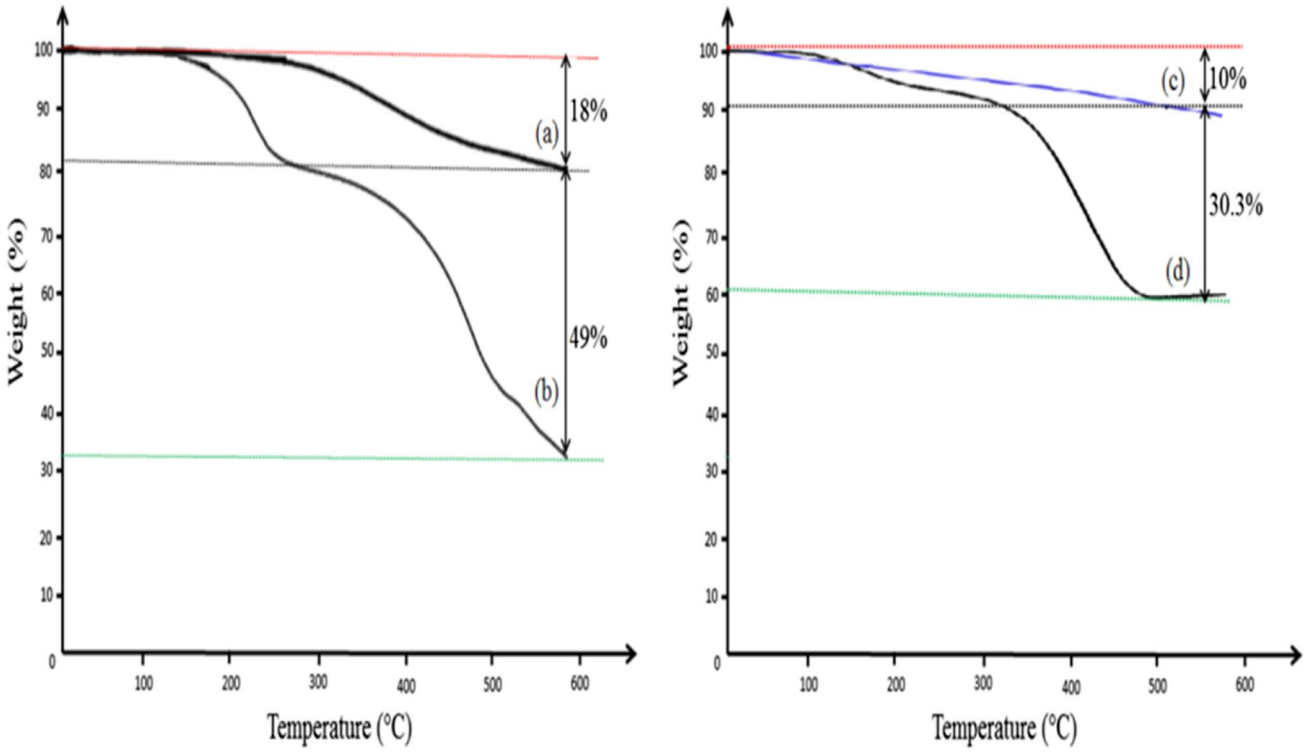

Fig. 6 TGA thermograms of *a* MWCNTs-COOH, *b* MWCNTs-SO_3H, *c* SWCNTs-COOH, *d* SWCNTs-SO_3H

so on [64]. Also, the weight loss between 200 and 600 °C is completely due to functional groups on the end and side wall of the CNTs. It is possible that these functional groups in this research are OH, COOH, and SO_3H groups. As shown in Fig. 6a, the attached COOH groups decomposed at about ~250 °C and 18 % weight was decreased. After treatment of the H_2SO_4 with MWCNTs-COOH, TGA of the MWCNTs-SO_3H showed that 49 % weight was deleted. Accordingly these results indicate that 67 % weight can be ascribed to the covalently of sulfonic and carboxylic acid groups to the side wall of the MWCNTs. The weight losses in the SWCNTs-COOH and SWCNTs-SO_3H were 10 and 30.3 % respectively. Taking into account that the covalently SO_3H measurements indicated one functionality every ~5 C atoms in the MWCNTs-SO_3H. Also, in the SWCNT the SO_3H functional groups measurements were shown one SO_3H every ~13 C atoms. Results obtained by TGA thermograms showed good agreement with results of FT-IR spectroscopy and Raman spectroscopy.

For calculation the extent of functionalization per C atoms, weight loss values were employed together with the molecular weight of the different groups and the Eq. (2) was applied [65]. Where X stands for the number of carbon atoms in the CNTs sample per each covalent functional group, R (%) is the residual mass at 600 °C in the TGA plot, L (%) is the weight loss in the range of 200 and 600 °C, and M_w is the molecular weight of the desorbed functional groups.

$$X = \frac{R(\%) \times M_w\left(\frac{g}{mol}\right)}{L(\%) \times 12\left(\frac{g}{mol}\right)} \quad (2)$$

Acidity measurement of the catalysts

Acid–base titration was employed to determine the density of sulfonic acid groups on the side wall of the MWCNTs-SO_3H and SWCNTs-SO_3H. The volume required to reach the neutral point was subtracted from the initial volume of NaOH used to obtain the volume of NaOH which has reacted with SO_3H group on the side wall MWCNTs (Eq. 3). The measurement was repeated three times for each sample and the average calculated. The acid–base titration showed that the amount of SO_3H attached to MWCNTs is 1.80 mmol g^{-1}. In addition, after preparation of MWCNTs-COOH, we calculate amount of –OH and –COOH by acid–base titration as described above. Acid–base titration for MWCNTs-COOH was 0.15 mmol g^{-1}. The acid–base titration results for the SWCNTs-SO_3H and SWCNTs-COOH were 0.94 and 0.10 mmol g^{-1} respectively.

$$\text{NaOH (mmol reacted with } SO_3H) = \text{NaOH (primary mmol)} - \text{NaOH (mmol unreacted with } SO_3H) \quad (3)$$

Table 1 The influence of the solvent on the *tert*-butylation of *p*-cresol

Entry	Solvent	MWCNTs-SO_3H				SWCNTs-SO_3H			
		Conv. *p*-cresol (%)[a]	2-TBC (%)[a]	2,6-DTBC (%)[a]	Other products[b] (%)[a]	Conv. *p*-cresol (%)[a]	2-TBC (%)[a]	2,6-DTBC (%)[a]	Other products[b] (%)[a]
1	*n*-hexane	50.7	29.8	17.4	3.5	51.3	26.8	17.8	6.7
2	$CHCl_3$	59.0	35.5	17.2	6.3	55.4	33.6	17.5	4.3
3	CH_3CN	68.8	50.4	16.8	1.6	66.7	44.9	16.8	5.0
4	CH_3NO_2	66.3	54.9	10.3	1.1	65.9	52.4	11.9	1.6
5[c]	Solvent-free	75.8	60.9	10.8	4.1	73.9	60.1	11.0	2.8

General reaction conditions: catalyst (25 mg), *T* reflux, *p*-cresol (5 mmol): MTBE (5 mmol) (1:1), solvent: 3 mL, Time: 10 h

[a] GC yields

[b] The other products are TBCE and oligomers

[c] General reaction conditions were same as previous experiments except temperature. $T = 70$ °C

Catalytic activity

In this research, we studied the influence of catalytic activity of MWCNTs-SO_3H and SWCNTs-SO_3H in the *tert*-butylation of *p*-cresol under different solvents, temperatures, molar ratios, amounts of the catalyst, and *tert*-butylation agent. In addition, we investigated recovery and reusability of the catalyst in this reaction.

The influence of the solvent in the tert-butylation of p-cresol

In order to choose the reaction media, different solvents were investigated in *tert*-butylation of *p*-cresol. Different solvents such as *n*-hexane, chloroform, acetonitrile, and nitromethane were chosen as the reaction medium (Table 1). Also the reaction was carried out under solvent-free conditions. We observed that from *n*-hexane to nitromethane the conversion of *p*-cresol was improved in *tert*-butylation of *p*-cresol catalyzed by MWCNTs-SO_3H and SWCNTs-SO_3H. The yield of 2-TBC was increased with increasing polarity of the solvents and the amounts of the other products were decreased to 1.1 and 1.6 % for MWCNTs-SO_3H and SWCNTs-SO_3H respectively (Table 1, entry 4). In addition, we checked the reaction under solvent-free conditions (Table 1, entry 5). In this condition, the yield of 2-TBC and conversion of *p*-cresol were improved. Hence, we choose the solvent-free conditions, because higher catalytic activity and selectivity were observed. It should be mentioned that the absence of organic solvent is in good agreement with green chemistry principles.

The influence of temperature in the tert-butylation of p-cresol under solvent-free conditions

The influence of the reaction temperature on the conversion of *p*-cresol and the selectivity to 2-TBC is shown in Table 2. The catalytic activity and selectivity of the MWCNTs-SO_3H and SWCNTs-SO_3H can be improved by increasing of temperature until 90 °C (Table 2).The reaction was carried out under different conditions. Depending on the reaction conditions and the nature catalytic system *tert*-butylation of *p*-cresol can be take place at the oxygen (*O*-alkylation) (TBCE) and/or at the ring carbon atoms (*C*-alkylation). The previous papers indicate that the selectivity is highly depending to the acid strength of the catalyst, the amount of the *tert*-butylating agent, and temperature too, which agrees with the results reported elsewhere [19, 20, 46]. In general, the *C*-alkylation requires stronger acid sites and higher temperature than for the *O*-alkylation. The conversion of *p*-cresol and the selectivity of 2-TBC reached maxima at 90 °C.

Table 2 The influence of temperature in the *tert*-butylation of *p*-cresol under solvent-free conditions

Entry	Temperature (°C)	MWCNTs-SO_3H				SWCNTs-SO_3H			
		Conv. *p*-cresol (%)[a]	2-TBC (%)[a]	2,6-DTBC (%)[a]	Other products[b] (%)[a]	Conv. *p*-cresol (%)[a]	2-TBC (%)[a]	2,6-DTBC (%)[a]	Other products[b] (%)[a]
1	50	54.3	33.3	2.9	18.1	47.5	29.8	7.8	9.9
2	70	75.8	60.9	4.1	10.8	73.9	60.1	2.8	11.0
3	90	82.9	70.7	8.8	3.4	77.1	68.7	6.1	2.3
4	100	85.1	69.3	7.1	8.7	83.4	68.1	9.2	6.1
5	120	84.3	64.1	9.2	11.0	82.8	60.0	12.1	10.7

General reaction conditions: catalyst (25 mg), *p*-cresol (5 mmol): MTBE (5 mmol) (1:1), solvent-free, Time: 10 h

[a] GC yields

[b] The other products are TBCE and oligomers

Table 3 The influence of molar ratio in the *tert*-butylation of *p*-cresol

Entry	Molar ratio (*p*-cresol: MTBE)	MWCNTs-SO_3H				SWCNTs-SO_3H			
		Conv. *p*-cresol (%)[a]	2-TBC (%)[a]	2,6-DTBC (%)[a]	Other products[b] (%)[a]	Conv. *p*-cresol (%)[a]	2-TBC (%)[a]	2,6-DTBC (%)[a]	Other products[b] (%)[a]
1	1:1	82.9	70.7	8.8	3.4	77.1	68.7	6.1	2.3
2	1:1.25	84.8	74.5	7.9	2.4	80.2	71.9	6.8	1.5
3	1:1.5	89.8	80.1	7.0	2.7	87.7	75.6	8.0	4.1
4	1:1.75	90.9	81.5	8.8	0.6	89.3	77.2	9.1	3.0
5	1:2	90.5	76.1	14.4	Trace	88.6	70.1	16.5	2.0

General reaction conditions: catalyst (25 mg), solvent-free, $T = 90$ °C, Time: 10 h

[a] GC yields

[b] The other products are TBCE and oligomers

The TBCE turn into 2-TBC at high temperature and a slightly further C-alkylation of 2-TBC was happened with MTBE. It also indicates that lower temperature favors the formation of TBCE, while higher temperature favors the formation of 2-TBC. We observed that at temperatures higher than 90 °C the conversion of *p*-cresol was improved, while the selectivity of the desired product (2-TBC) was decreased for two types of catalysts (Table 2, entries 4, 5). Hence, we chose 90 °C as optimum temperature.

The influence of molar ratio in the tert-butylation of p-cresol under solvent-free conditions

Table 3 shows the effect of the molar ratio *p*-cresol: MTBE on the catalytic activity and selectivity of MWCNTs-SO_3H and SWCNTs-SO_3H in *tert*-butylation of *p*-cresol at 90 °C under solvent-free conditions. All of the results are summarized in Table 3. Conversion of the *p*-cresol increases with the *p*-cresol:MTBE molar ratio up to 1:2, which has been ascribed to the preferential adsorption of MTBE on the BrØnsted acid sites as compared with iso-butene (from *tert*-butyl carbocation). However, further increases of *p*-cresol:MTBE molar ratio to 1:1.5, result in an increasing yield of 2-TBC. But the selectivity for 2-TBC decreases with increasing *p*-cresol: MTBE molar ratio, while the selectivity 2,6-DTBC increases. This is due to a higher concentration of the alkylating agent in the reaction medium, which facilitates the formation of the dialkylated product. The best molar ratio was 1:1.5.

The influence of the amount of catalyst in the tert-butylation of p-cresol under solvent-free conditions

The catalytic activity and selectivity of MWCNTs-SO_3H and SWCNTs-SO_3H at different amounts of the catalyst are shown in Table 4. As the amount of the catalyst increase, both the conversion of *p*-cresol and the selectivity to 2-TBC first increase and then reach a steady state. The selectivity

Table 4 The influence amount of the catalyst in the *tert*-butylation of *p*-cresol

Entry	Catalyst (mg)	MWCNTs-SO_3H				SWCNTs-SO_3H			
		Conv. *p*-cresol (%)[a]	2-TBC (%)[a]	2,6-DTBC (%)[a]	Other products[b] (%)[a]	Conv. *p*-cresol (%)[a]	2-TBC (%)[a]	2,6-DTBC (%)[a]	Other products[b] (%)[a]
1[c]	–	–	–	–	–	–	–	–	–
2	10	25.2	6.0	5.1	14.1	20.1	4.1	6.5	9.5
3	15	33.3	17.8	10.1	5.4	29.3	18.3	8.8	2.2
4	20	55.1	43.7	9.7	1.7	54.9	41.8	8.9	4.2
5	25	89.8	80.1	7.0	2.7	87.7	75.6	8.0	4.1
6	30	94.1	91.1	2.3	0.7	87.3	79.1	4.3	3.9
7	35	94.5	91.3	2.5	0.7	92.2	88.2	3.1	0.9

General reaction conditions: *p*-cresol (5 mmol): MTBE (7.5 mmol) (1:1.5), solvent-free, $T = 90$ °C, Time: 10 h

[a] GC yields

[b] The other products are TBCE and oligomers

[c] Time: 48 h

Table 5 The influence of alkylating agent in the *tert*-butylation of *p*-cresol

Entry	*tert*-butylation agent	MWCNTs-SO_3H[a]				SWCNTs-SO_3H[b]			
		Conv. *p*-cresol (%)[c]	2-TBC (%)[c]	2,6-DTBC (%)[c]	Other products[d] (%)[c]	Conv. *p*-cresol (%)[c]	2-TBC (%)[c]	2,6-DTBC (%)[c]	Other products[d] (%)[c]
1	MTBE	94.1	91.1	2.3	0.7	92.2	88.2	3.1	0.9
2	*tert*-BuOH	94.5	85.6	6.7	2.2	91.8	81.4	7.7	2.7

[a] General reaction conditions: catalyst (30 mg), *p*-cresol (5 mmol): MTBE (7.5 mmol) (1:1.5), solvent-free, $T = 90$ °C, Time: 10 h

[b] General reaction conditions: catalyst (35 mg), *p*-cresol (5 mmol): MTBE (7.5 mmol) (1:1.5), solvent-free, $T = 90$ °C, Time: 10 h

[c] GC yields

[d] The other products are TBCE and oligomers

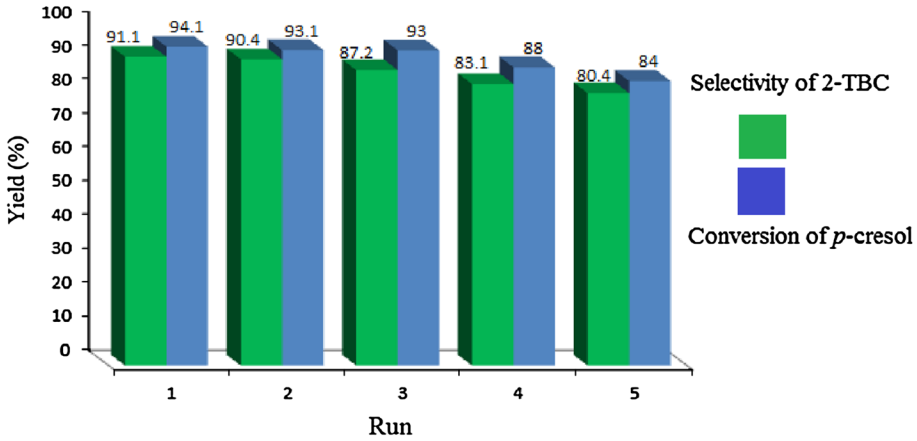

Fig. 7 The reusability of the MWCNTs-SO_3H

to 2,6-DTBC decreases. However, a strong acid system does not lead to further alkylation of 2-TBC with MTBE. The highest conversion of *p*-cresol and selectivity of 2-TBC were observed using 30 and 35 mg catalyst for MWCNTs-SO_3H and SWCNTs-SO_3H respectively (Table 4, entries 6, 7). In addition, it is well known that in the absence of the catalyst, the reaction was not carried out (Table 4, entry 1).

The influence of alkylating agent in the tert-butylation of p-cresol under solvent-free conditions

In this part, we investigated the influence of alkylating agent in the catalytic activity and selectivity of the catalyst (Table 5). We observed that MTBE for two types of the catalyst are suitable while *tert*-BuOH decreased the selectivity of the 2-TBC.

Scheme 3 The proposed reaction mechanism

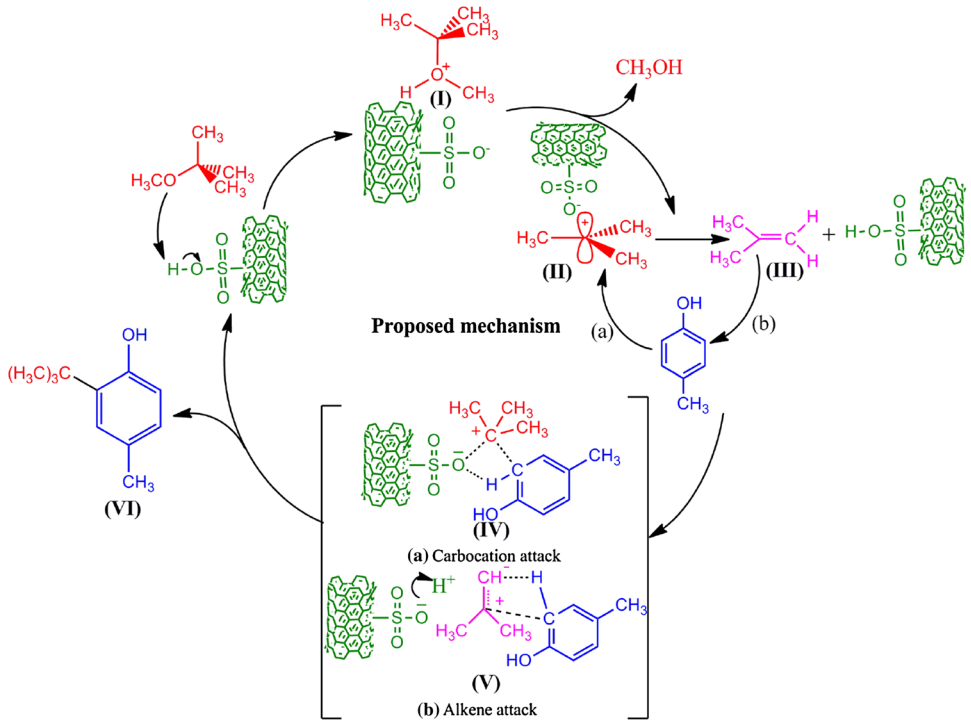

Table 6 Comparison of the results obtained for the *tert*-butylation of *p*-cresol catalyzed by CNTs-SO_3H with those obtained by the recently reported catalyst

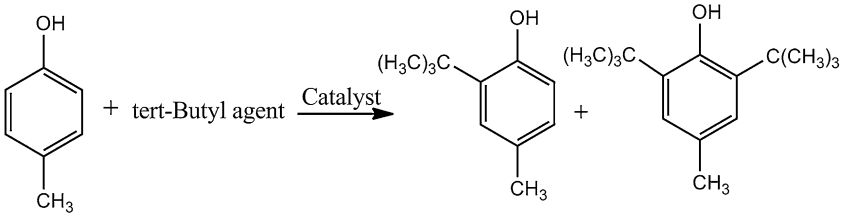

Entry	Catalyst	*T* (°C)	Conversion of *p*-cresol (%)	Yield (%)		Ref.
				2-TBC	2,6-DTBC	
1	HPW@MCM-41	110	85	78	6.7	[47]
2	K10-FeAl20	80	–	86.7	1.7	[20]
3	TPA@ZrO_2	100	61	81.4	18.1	[43]
4	Zn-Al-MCM-41	120	93.2	98.6	–	[48]
5	TPA@TiO_2	130	82	89.5	7.5	[40]
6	WO_x-ZrO_2	130	69.8	92.4	6.3	[44]
7	Al-MCM-41	90	88.2	90.4	–	[49]
8	Ionic Liquid-SO_3H	70	80	90	9.5	[36]
9	$Cu_{1-x}Co_xFe_2O_4$	100	70	100	0	[52]
10	12-TPA-ZrO_2	80	83	97	–	[46]
11	MWCNTs-SO_3H	90	94.1	91.1	2.3	This work
12	SWCNTs-SO_3H	90	92.2	88.2	3.1	This work

The reusability and stability of the catalyst

For practical applications of a heterogeneous catalyst, level of reusability is a very important feature. The homogeneous acidic catalyst do not recovered even one time, in contrast the CNTs-SO_3H catalyst can be filtered and reuse several times without significant loss of its catalytic activity. We examined the reusability of the MWCNTs-SO_3H in the

multiple sequential reaction of *p*-cresol and MTBE (Fig. 7). After each run, the catalyst was isolated by filtration, washed exhaustively with chloroform, deionized water and ethanol, and it dried at 80 °C for 10 h before being used with fresh *p*-cresol and MTBE.

The proposed reaction mechanism

The suggested mechanism in Scheme 3 seems to be reasonable for the *tert*-butylation of *p*-cresol with MTBE catalyzed by CNTs-SO_3H under solvent-free conditions. The methoxy group in MTBE is first activated by protonation with CNTs-SO_3H to give **I**. The oxonium ion can easily liberate CH_3OH molecule to form **II**. The carbocation **II** on the catalyst can also undergo elimination of proton to form the alkene **III**. The formed carbocation could directly attack the *ortho* position of *p*-cresol via formation of transition state (a). The alkene (**III**) could also attack the *ortho* position of *p*-cresol via formation of transition state (b). The attack of (**II**) and (**III**) on the *p*-cresol gives the species (**IV**) and (**V**), respectively, which is subsequently converted to the 2-TBC (**VI**) and release CNTs-SO_3H for the next catalytic cycle.

Performing of the reaction in the scale-up

In order to show the practical applicability of the CNTs-SO_3H, we have scaled up the reaction of *p*-cresol (50 mmol), MTBE (75 mmol) and MWCNTs-SO_3H (300 mg) under similar optimized reaction conditions. The reaction proceeds well with 93 % isolated yields of the 2-TBC at 10 h.

Comparison of the obtained results with recently reported catalysts in the tert-butylation of p-cresol

In order to show the efficiency and advantage of the new method in the synthesis of 2-TBC, we have compared the obtained results in the *tert*-butylation of *p*-cresol catalyzed by CNTs-SO_3H with those of some reported methods in the literature (Table 6). It seems that the presented new method is superior in terms of product yield and selectivity, reusability of the catalyst, un-deactivation of the catalyst, and solvent-free conditions.

Conclusions

In conclusions, efficient, heterogeneous, and reusable MWCNTs-SO_3H and SWCNTs-SO_3H were prepared via chemical process. The catalysts were characterized by SEM, FT-IR spectroscopy, Raman spectroscopy, TGA, and acid–base titration. On the basis of the above observations, we conclude that the excellent catalytic activity and selectivity of the MWCNTs-SO_3H and SWCNTs-SO_3H can be correlated to solvent, temperature, molar ratio, amount of the catalyst, and alkylating agent. We observed that the best conditions for the catalytic activity and selectivity of MWCNTs-SO_3H are at 90 °C, molar ratio (1:1.5), catalyst 30 mg, 10 h, MTBE as alkylating agent, and solvent-free conditions. Also, the best conditions for SWCNTs-SO_3H are as the same conditions for the MWCNTs-SO_3H. But the amount of the SWCNTs-SO_3H is 35 mg. The results showed that in this reaction the MWCNTs-SO_3H is a little better than SWCNTs-SO_3H, because the acid strength of the MWCNTs-SO_3H was higher than SWCNTs-SO_3H. We also investigated the recycling of the MWCNTs-SO_3H and it reused in five consecutive runs and showed slight decrease of the catalytic activity, selectivity and conversion of *p*-cresol after each recycling. In addition we carried out *tert*-butylation of *p*-cresol in the scale-up.

Acknowledgments We gratefully acknowledge the financial support by Malek-Ashtar University of Technology (MUT). We thank Dr. Rashidi in Research Institute of Petroleum Industry (RIPI) for useful help.

References

1. P.T. Anastas, M.M. Kirchhoff, Acc. Chem. Res. **35**, 686 (2002)
2. J.H. Clark, Acc. Chem. Res. **35**, 791 (2002)
3. H.T. Gomes, S.M. Miranda, M.J. Sampaio, A.M.T. Silva, J.L. Faria, Catal. Today **151**, 153 (2010)
4. A. Takagaki, M. Toda, M. Okamura, J.N. Kondo, S. Hayashi, K. Domen, M. Hara, Catal. Today **116**, 157 (2006)
5. X. Liang, M. Zeng, C. Qi, Carbon **48**, 1844 (2010)
6. H. Xiao, Y. Guo, X. Liang, C. Qi, J. Solid State Chem. **183**, 1721 (2010)
7. Y. Zhao, H. Wang, Y. Zhao, J. Shen, Catal. Commun. **11**, 824 (2010)
8. V. Mirkhani, M. Moghadam, S. Tangestaninejad, I. Mohammadpoor-Baltork, M. Mahdavi, Monatsh. Chem. **140**, 1489 (2009)
9. J. Safari, S. Gandomi-Ravandi, J. Mol. Catal. A: Chem. **373**, 72 (2013)
10. X. Hu, Y.-Y. Zhang, K. Tang, G.-L. Zou, Synth. Met. **150**, 1 (2005)
11. Y. Wang, Z. Iqbal, S. Mitra, J. Am. Chem. Soc. **128**, 95 (2005)
12. H. Yu, Y. Jin, Z. Li, F. Peng, H. Wang, J. Solid State Chem. **181**, 432 (2008)
13. L. Adams, A. Oki, T. Grady, H. McWhinney, Z. Luo, Phys **E41**, 723 (2009)
14. M.M. Doroodmand, S. Sobhani, A. Ashoori, Can. J. Chem. **90**, 701 (2012)
15. F. Peng, L. Zhang, H. Wang, P. Lv, H. Yu, Carbon **43**, 2405 (2005)
16. J. Pospíšil, Polym. Degrad. Stab. **20**, 181 (1988)
17. J. Murphy, in *Additives for Plastics Handbook*, 2nd edn., ed. by J. Murphy (Elsevier Science, Amsterdam, 2001)
18. N. Platzer, J. Polym. Sci. Pol. Lett. **24**, 659 (1986)
19. S.E. Dapurkar, P. Selvam, Appl. Catal. **A254**, 239 (2003)
20. A.B. Shinde, N.B. Shrigadi, S.D. Samant, Appl. Catal. **A276**, 5 (2004)
21. D. Mravec, P. Zavadan, A. Kaszonyi, J. Joffre, P. Moreau, Appl. Catal. **A257**, 49 (2004)

22. G. Kostrab, M. Lovič, I. Janotka, M. Bajus, D. Mravec, Appl. Catal. **A323**, 210 (2007)
23. E. Dumitriu, V. Hulea, J. Catal. **218**, 249 (2003)
24. G. Kostrab, M. Lovič, A. Turan, P. Hudec, A. Kaszonyi, M. Bajus, J. Uhlár, P. Lehocký, D. Mravec, Catal. Commun. **18**, 176 (2012)
25. G. Kamalakar, K. Komura, Y. Sugi, Ind. Eng. Chem. Res. **45**, 6118 (2006)
26. H.-J. Dong, L. Shi, Ind. Eng. Chem. Res. **49**, 2091 (2010)
27. L.-B. Chen, H.-j Dong, L. Shi, Ind. Eng. Chem. Res. **49**, 7234 (2010)
28. A. Vinu, K.U. Nandhini, V. Murugesan, W. Böhlmann, V. Umamaheswari, A. Pöppl, M. Hartmann, Appl. Catal. **A265**, 1 (2004)
29. T. Mathew, S. Shylesh, B.M. Devassy, M. Vijayaraj, C.V.V. Satyanarayana, B.S. Rao, C.S. Gopinath, Appl. Catal. **A273**, 35 (2004)
30. A. Vinu, B.M. Devassy, S.B. Halligudi, W. Böhlmann, M. Hartmann, Appl. Catal. **A281**, 207 (2005)
31. G.S. Kumar, M. Vishnuvarthan, M. Palanichamy, V. Murugesan, J. Mol. Catal. A: Chem. **260**, 49 (2006)
32. B. Rác, M. Nagy, I. Pálinkó, Á. Molnár, Appl. Catal. **A316**, 152 (2007)
33. E.-P. Ng, H. Nur, K.-L. Wong, M.N.M. Muhid, H. Hamdan, Appl. Catal. **A323**, 58 (2007)
34. E.-P. Ng, S.N. Mohd Subari, O. Marie, R.R. Mukti, J.-C. Juan, Appl. Catal. **A450**, 34 (2013)
35. X. Liu, M. Liu, X. Guo, J. Zhou, Catal. Commun. **9**, 1 (2008)
36. K. Kondamudi, P. Elavarasan, P.J. Dyson, S. Upadhyayula, J. Mol. Catal. A: Chem. **321**, 34 (2010)
37. P. Elavarasan, K. Kondamudi, S. Upadhyayula, Chem. Eng. J. **166**, 340 (2011)
38. X. Liu, J. Zhou, X. Guo, M. Liu, X. Ma, C. Song, C. Wang, Ind. Eng. Chem. Res. **47**, 5298 (2008)
39. F. Adam, K.M. Hello, T.H. Ali, Appl. Catal. **A399**, 42 (2011)
40. S.M. Kumbar, G.V. Shanbhag, F. Lefebvre, S.B. Halligudi, J. Mol. Catal. A: Chem. **256**, 324 (2006)
41. B.M. Reddy, M.K. Patil, G.K. Reddy, B.T. Reddy, K.N. Rao, Appl. Catal. **A332**, 183 (2007)
42. B.M. Devassy, G.V. Shanbhag, S.P. Mirajkar, W. Böhringer, J. Fletcher, S.B. Halligudi, J. Mol. Catal. A: Chem. **233**, 141 (2005)
43. B.M. Devassy, G.V. Shanbhag, F. Lefebvre, S.B. Halligudi, J. Mol. Catal. A: Chem. **210**, 125 (2004)
44. S. Sarish, B.M. Devassy, S.B. Halligudi, J. Mol. Catal. A: Chem. **235**, 44 (2005)
45. B.M. Devassy, G.V. Shanbhag, S.B. Halligudi, J. Mol. Catal. A: Chem. **247**, 162 (2006)
46. N. Bhatt, P. Sharma, A. Patel, P. Selvam, Catal. Commun. **9**, 1545 (2008)
47. G. Kamalakar, K. Komura, Y. Sugi, Appl. Catal. **A310**, 155 (2006)
48. M. Selvaraj, P.K. Sinha, J. Mol. Catal. A: Chem. **264**, 44 (2007)
49. M. Selvaraj, S. Kawi, Micropor. Mesopor. Mat. **98**, 143 (2007)
50. R.C. Huston, W.C. Lewis, J. Am. Chem. Soc. **53**, 2379 (1931)
51. H. Hart, E.A. Haglund, J. Org. Chem. **15**, 396 (1950)
52. R. Alamdari, Z. Hosseinabadi, M. Khouzani, J. Chem. Sci. **124**, 827 (2012)
53. R. Fareghi-Alamdari, M. Golestanzadeh, F. Agend, N. Zekri, J. Chem. Sci. **125**, 1185 (2013)
54. R. Fareghi-Alamdari, M. Golestanzadeh, F. Agend, N. Zekri, C. R. Chimie **16**, 878 (2013)
55. R. Fareghi-Alamdari, M. Golestanzadeh, F. Agend, N. Zekri, Can. J. Chem. **91**, 982 (2013)
56. H. Hu, P. Bhowmik, B. Zhao, M.A. Hamon, M.E. Itkis, R.C. Haddon, Chem. Phys. Lett. **345**, 25 (2001)
57. N.P. Blanchard, R.A. Hatton, S.R.P. Silva, Chem. Phys. Lett. **434**, 92 (2007)
58. A.G. Osorio, I.C.L. Silveira, V.L. Bueno, C.P. Bergmann, Appl. Surf. Sci. **255**, 2485 (2008)
59. H. Peng, L.B. Alemany, J.L. Margrave, V.N. Khabashesku, J. Am. Chem. Soc. **125**, 15174 (2003)
60. H. Hu, B. Zhao, M.E. Itkis, R.C. Haddon, J. Phys. Chem. **B107**, 13838 (2003)
61. S. Goyanes, G.R. Rubiolo, A. Salazar, A. Jimeno, M.A. Corcuera, I. Mondragon, Diamond Relat. Mater. **16**, 412 (2007)
62. A. Jorio, M.A. Pimenta, A.G.S. Filho, R. Saito, G. Dresselhaus, M.S. Dresselhaus, New J. Phys. **5**, 139 (2003)
63. E. Flahaut, C. Laurent, A. Peigney, Carbon **43**, 375 (2005)
64. J.J. Stephenson, J.L. Hudson, S. Azad, J.M. Tour, Chem. Mater. **18**, 374 (2005)
65. J.M. González-Domínguez, M. González, A. Ansón-Casaos, A.M. Díez-Pascual, M.A. Gómez, M.T. Martínez, J. Phys. Chem. **C115**, 7238 (2011)